Session 12

Experimental Data

Reconciling Numerical Simulations with Wind-Tunnel Experiments in Hypersonic Flows

[1]Yuan Jia; [1]Qiao Zhang; [2]Hao Ma*; [1]Guoqin Zhao; [1]Chi Zhang; [1]Chih-Yung Wen*.

[1] *Department of Aeronautical and Aviation Engineering, The Hong Kong Polytechnic University, Kowloon, Hong Kong, 999077, China*

[2]*School of Aerospace Engineering, Zhengzhou University of Aeronautics, Zhengzhou, 450046, China*

Abstract

Discrepancies between numerical simulations and wind-tunnel experiments are a key bottleneck for high-fidelity aerodynamic design and validation. This study establishes an analytical framework to not only quantify but also predict the discrepancies in hypersonic flow over a compression ramp, arising from both geometric imperfections and unquantified freestream noise in a wind tunnel. The primary objective is to bridge the simulation-experiment gap, thereby enhancing CFD's predictive capability under real experimental conditions. Experimentally, density fields from schlieren imaging are compared with high-fidelity CFD across ten test cases to establish baseline differences. This is followed by a statistical fitting analysis encompassing 22 datasets, including repeated experiments, using time-averaged schlieren data. To advance predictive capability, a data-driven model is developed leveraging sequences of 60 instantaneous schlieren images per test case. The proposed framework provides a systematic pathway for reconciling simulation and experimental data, thereby enhancing the credibility of CFD predictions for complex hypersonic flows. To further bridge the gap between simulated and experimental domains, a two-stage deep learning adaptation strategy is also introduced. First, a foundational deep learning model is trained using both CFD and experimental data to learn basic flow-field characteristics; subsequently, the model is fine-tuned with experimental data to better adapt to the experimental domain, during which intermediate feature representations are extracted. By extracting and incorporating feature-level differences between CFD and experiments, the model's generalization to real experimental scenarios is enhanced, ultimately enabling the derivation of more accurate, experiment-matched flow-field parameters from CFD-based simulations.

Keywords: Hypersonic flow, Compression ramp, Wind-tunnel experiment, Numerical simulation, Fine-tuning

Automated Image-Based Classification of Air Lubrication Flow Regimes Using Deep Learning

[1]Semanur Kucuk*; [2]Cosimo Della Santina; [1]Angeliki Laskari;

[1] Process & Energy, TU Delft Mechanical Engineering

[2]Cognitive Robotics, TU Delft Mechanical Engineering

Abstract

Air lubrication is an effective method for reducing fuel consumption in marine applications. Depending on the air injection rate and flow conditions, three distinct air phase regimes are observed along the hull surface: a bubbly regime, a transitional regime, and an air layer regime. Among these, the air layer regime yields the highest drag reduction, with reported efficiencies approaching 80 percent. However, sustaining this regime generally requires increased air supply, resulting in higher auxiliary power demand. Therefore, accurate identification of the governing flow regime is essential for evaluating air lubrication performance. In many experimental studies, this classification is still performed manually based on visual inspection, which limits reproducibility and scalability. In this work, an automated image-based classification approach is presented to distinguish between bubbly, transition, and air layer regimes. A ResNet50 convolutional neural network is trained using transfer learning on labeled experimental images acquired under varying operating conditions. The proposed approach enables consistent regime identification across large datasets and provides a scalable basis for systematic analysis of air lubrication experiments.

Keywords: air lubrication, flow regime identification, image classification, drag reduction

PeakCNN for particle image localization: Examples, variations, and improvements

[1]Philipp Godbersen*; [1]Daniel Schanz; [1,2]Andreas Schröder

[1]*Institute of Aerodynamics and Flow Technology, German Aerospace Center (DLR), Germany*

[2]*Brandenburgisch Technische Universität (BTU) Cottbus-Senftenberg, Germany*

Abstract

Lagrangian Particle Tracking (LPT) methods for flow measurements such as Shake-the-Box [1] (STB) rely on the accurate 2D localization of particle images on camera images (‘peak detection’) as a first step of reconstructing their 3d positions via triangulation procedures using the peaks of multiple cameras. This is particularly important for the measurement of dense particle clouds where particle images strongly overlap on the cameras and accurate detection of them is a challenge. PeakCNN [2] is a supervised learning approach based on Convolutional Neural Networks (CNNs) and allows to find correct particle image positions even with strong overlaps, enabling reconstruction of particle clouds at higher particle densities than possible before. Its key feature lies in its single stage nature whereby subpixel accurate positions are obtained from images directly with one model inspired by the YOLO approach, as opposed to separate models acting on detected image patches similar to a R-CNN approach.

The PeakCNN method has shown significant improvement over conventional peak detectors on a variety of synthetic and real-world experiments, including its use in the DLR submission to the recent 2nd Challenge on LPT and Data Assimilation, where very high seeding densities were successfully handled. Additionally, several variations and improvements have since been developed extending the original concept, such as a partly pre-solved peak detection or inclusion of other additional information from the tracking scheme itself. The neural network based approach makes it possible to include additional information into the process such as confidence of track accuracy or other quantities, something that would be difficult to include in a conventional peak detection algorithm. The submission will include an introduction to the method, showcase its performance and ease of use on several cases with an emphasis on the novel developments regarding greater integration into the LPT method.

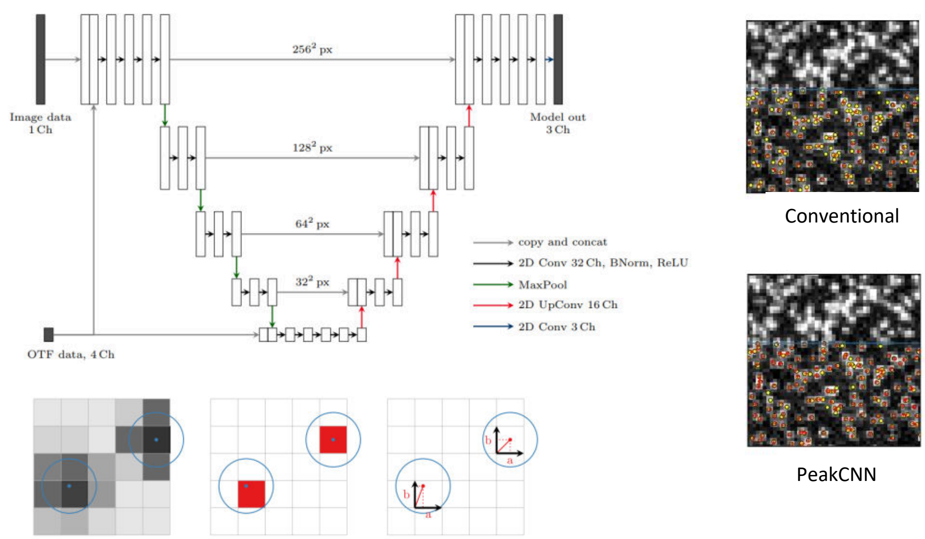

Figure 1 (left) PeakCNN architecture with single stage processing. (right) example of detection performance with ground truth in yellow and detections in red markers.

References

[1] D. Schanz, S. Gesemann und A. Schröder, „Shake-The-Box: Lagrangian particle tracking at high particle image densities,“ *Experiments in Fluids,* Bd. 57, Nr. 5, 2016.

[2] P. Godbersen, D. Schanz und A. Schröder, „Peak-CNN: improved particle image localization using single-stage CNNs,“ *Experiments in Fluids,* Bd. 65, Nr. 10, 2024.

Keywords: Particle image detection, PeakCNN, Shake-The-Box, Particle tracking,

Proceedings of the 1st international Symposium on AI and Fluid Mechanics
Paper No [leave blank]

LGFNet: Local-Global Fusion Network for Multi-Source Aerodynamics

[1]Qinye Zhu; [1]Yu Xiang*; [1]Jun Zhang; [1]Wenyong Wang;

[1]*School of Computer Science and Engineering, University of Electronic Science and Technology of China, Chengdu, China*

Abstract

In the field of aerodynamic data fusion, the effective fusion of Computational Fluid Dynamic (CFD) simulation, wind tunnel tests, and flight tests data of various sources represents a critical approach to improve the accuracy and reliability of aerodynamic characteristic prediction, which is also fundamental to the design of aircraft control systems and the optimization of overall performance. We propose Local-Global Fusion Network (LGFNet) to advance this field. Within its three layers, the Spatial Perception Layer employs a sliding-window mechanism to capture and reinforce continuous local features. The Relational Reasoning Layer then integrates a self-attention mechanism to dynamically weigh global data relationships, effectively strengthening long-range correlations. Finally, the Feature Synthesis Layer bridges these fine-grained details with global context via skip connections to achieve high-fidelity aerodynamic prediction. By bridging fine-grained details with global context, LGFNet achieves superior feature integration. Experiments on two datasets demonstrate that LGFNet significantly reduces uncertainty in aerodynamic force coefficients, achieving state-of-the-art (SOTA) performance.

Keywords: multi-source aerodynamic data; local-global fusion; self-attention mechanism

Introduction

In contemporary aerospace engineering, acquiring high-fidelity aerodynamic data is fundamental to aircraft design, flight envelope expansion, and performance evaluation [1]. Furthermore, robust aerodynamic modeling is indispensable for accurate parameter identification and the synthesis of resilient flight control systems [2][3]. Currently, the principal paradigms for aerodynamic data acquisition encompass Computational Fluid Dynamic (CFD) simulations, wind tunnel experiments, and empirical flight tests. Although CFD approaches efficiently generate high-volume datasets, their predictive accuracy is frequently compromised by underlying theoretical assumptions and computational resource bottlenecks. Conversely, while wind tunnel experiments yield precise data within controlled environments, they are resource-intensive and lack scalability due to the prerequisite of physical prototypes. Ultimately, flight tests provide ground-truth data for high-fidelity validation; however, their practical utility is fundamentally constrained by prohibitive costs, extended operational lifecycles, and stringent boundary condition limitations [4]-[6].

Machine learning effectively extracts complex features and addresses nonlinearities, driving significant progress in multi-source data fusion (MDF) in recent years [3][7][12]. Specifically, architectures such as XGBoost[13], composite NNs[14], and RBFGANs[6] have demonstrated remarkable fusion performance. However, these methods struggle to capture global, long-range information [15]. While the self-attention mechanism resolves this by effectively capturing long-range dependencies [16][18], its aerodynamic application is hindered by a lack of local information capture and high computational demands [19].

Based on the above studies, we propose LGFNet (Local-Global Fusion Network). The contributions are as follows:

1) Based on multi-scale data features extraction, we adopt sliding window method to enhance the extraction of local features, and at the same time introduce self-attention mechanism to improve the learning of long-range features, thereby achieving better performances for feature capture and fusion of multi-source aerodynamic data.

2) A novel LGFNet model with data alignment module, LGFNet module based on the above method and mechanism is proposed.

3) Experimental results showed that LGFNet effectively fused multi-source aerodynamic data, not only highly matched the high-fidelity flight test data, but also retained the trend of lower-fidelity CFD data together with successfully decreased the data uncertainty.

*Corresponding Author, E. Stavropoulos-Vasilakis evangelos.stavropoulos-vasilakis@city.ac.uk

Numerical Method

Relevant definitions and Overview

We first make the following definitions in Table 1.

Table 1. Relevant Definitions

Symbol	Definition
	Aerodynamic states
	Aerodynamic forces
	The dimension of aerodynamic states
	The dimension of aerodynamic forces
	The dimension of a data
	The number of the low or high fidelity data
	The number of data in the aligned dataset
,	Original low or high-fidelity dataset
	The aligned low or high-fidelity dataset
L , S_{tr}	Sliding window size and stride
	The dimension of a data in the aligned sub-dataset

Original dataset can be expressed as:

is a data vector, where represents the number of dataset samples of the -th dataset.

The LGFNet is composed of a Data Alignment Module and a LGFNet Core Module. The core module integrates three specialized layers: the SPL establishes a sliding-window mechanism to reinforce the coverage and sequential continuity of local features; the RRL intro duces a self-attention mechanism to strengthen long-range dependencies by dynamically weighing global data relationships; and the FSL reconstructs high-fidelity responses via skip connections to preserve fine-grained details. The overview is shown in Figure 1.

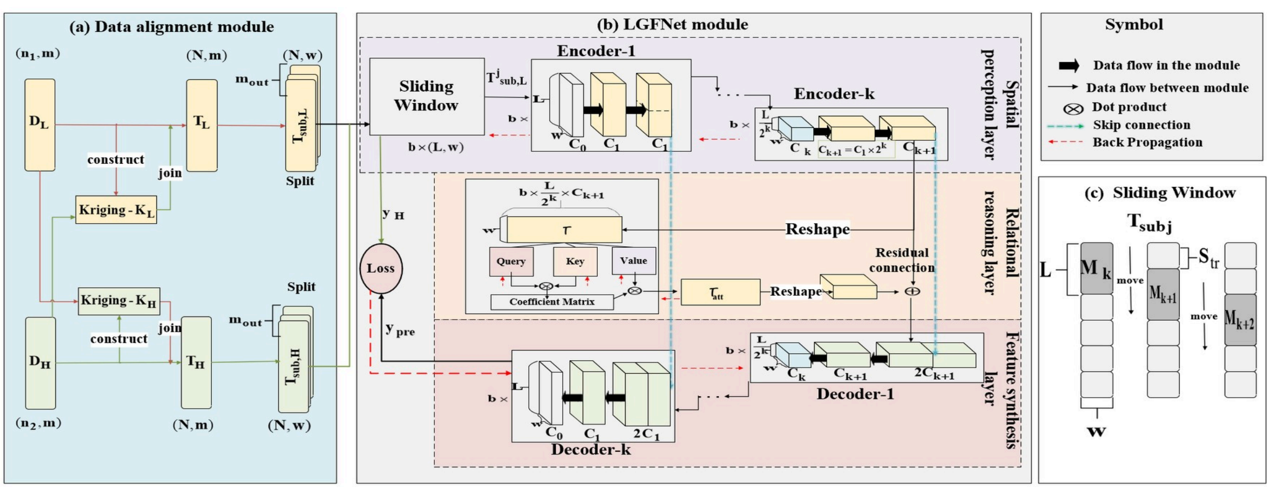

Figure 1 The overview of the aerodynamic data fusion method we proposed, (a) shows data alignment preprocessing and (b) shows the three layers of LGFNet model.

Data alignment module

Since , we employ Kriging interpolation [20] to align the original datasets and into and with the same aerodynamic states . As shown in Figure 1a, For and , interpolation models and are constructed. By defining the state sets and , cross-interpolation is performed as follows: for and for . To avoid the poor extrapolation ability of the Kriging model [21], the aligned datasets and are strictly bounded by , which is the intersection of the numerical ranges of and . Since

*Corresponding Author, E. Stavropoulos-Vasilakis evangelos.stavropoulos-vasilakis@city.ac.uk

aerodynamic forces are independent,   are decomposed into sub-datasets () and used as the input () and label (of LGFNet module.

LGFNet module

Spatial perception layer (SPL)

Each sub-dataset is segmented using sliding windows of size with stride , generating   blocks: , , SW is shown in Figure 1c. It not only addresses the memory limitation issue but also provides contextual continuity through the overlap of data blocks, enabling the model to learn the correlation between local and global features. Let the batch size be , the batch tensor can be represented as , where denotes the index in the batch, the second dimension of signifies the number of the input channel. SPL consists of an initial double convolutional layer followed by downsampling layers. Define the output of each layer is , and . Each downsampling module applies:

where channels double () and height halves (). The output of SPL is ,where .

Relational reasoning layer (RRL)

SPL mainly realizes the local feature extraction of pieces of data within the window. However, the long-range dependencies among the data have become the key bottleneck restricting the fusion effect. Therefore, we introduce RRL and apply a self-attention mechanism. , is reshaped into a three-dimensional tensor ,where ; thus, this new tensor encompasses the information of all data points within a single training iteration. Multi-head self-attention is applied:

represents the sine and cosine position encoding of . denotes the dimension of the key vector. is the final linear projection layer of multi-head attention.

The query tensor represents the aerodynamic data which similarity should be sought at present, and the key tensor represents the characteristic index of the aerodynamic data. calculates the similarity or correlation strength among different aerodynamic data, reflecting the intensity of concern among all the data. represents the actual information content of aerodynamic data and stores the aerodynamic force coefficient characteristics under specific aerodynamic conditions. integrates all the correlation information of the data. After reshaping back to , a residual connection yields: , Then serves as the input to FSL.

Feature synthesis layer (FSL)

FSL comprises decoder layers , each decoder layer includes bilinear interpolation upsampling, skip connection with the corresponding layer of the SPL, two consecutive convolution operations similar to the SPL:
where denotes concatenation.

Finally, a convolutional layer is applied to adjust the number of channels to , yielding the final output . The loss function minimizes the difference between predicted () and high-fidelity () forces:

Results

Dataset Description

Data from two aircraft models (CARDC) were used. Dataset 1 comprises CFD (: 38,116 samples) and flight test (: 16,983 samples) data. Dataset 2 comprises CFD (: 600 samples) and wind tunnel (: 710 samples) data. States include ,

*Corresponding Author, E. Stavropoulos-Vasilakis evangelos.stavropoulos-vasilakis@city.ac.uk

predicting forces , and . is Mach number, is angle of attack, is sideslip angle, , and are control surface deflections. is axial force coefficient, is normal force coefficient and is lateral force coefficient.

Comparison Experiments

LGFNet was benchmarked against models by mode1 Lin [13], model 2 He [14], and mode 3 Hu [6] over 20 iterations using multiple random seeds. Figure 2 compares 2D fusion curves of four models for , and aerodynamic forces on the same sample sequence segment of Dataset 1. It can be seen that the model fusion curve is very close to the FLI curve, losing the CFD trend. This proves that although its MSE is small (it can be seen from the subsequent table 2), it fails to learn the CFD trend. model 3 fusion curve jitter is obvious, in contrast, both the red LGFNet fusion curve and the model 2 fusion curve are closer to the FLI curve while retaining the trend of the CFD curve. However, from the e local emphasis, the fusion effect of the red LGFNet curve is better.

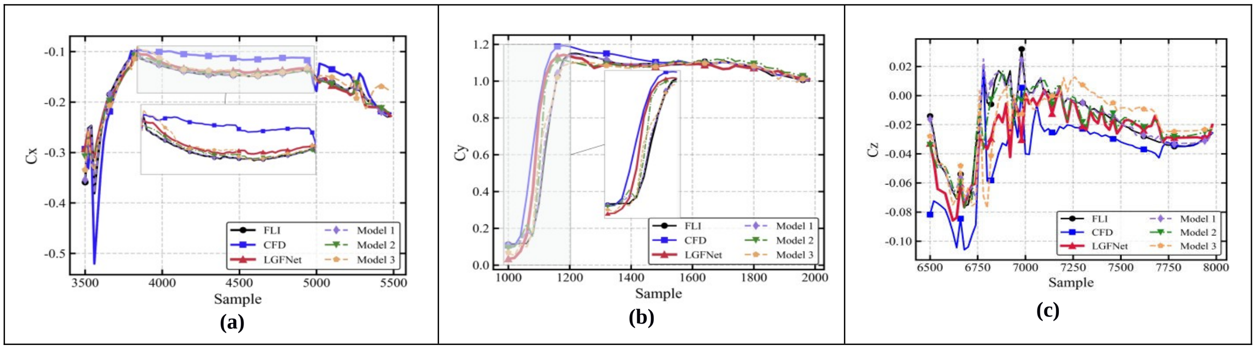

Figure 2 The comparisons of , and with CFD and FLI for Dataset 1 by the four models (The red dotted box is for local emphasis.).

As shown in Table 2 and Table 3, LGFNet achieves the lowest uncertainty across almost all aerodynamic coefficients, verifying its superior stability and reliability.

Table 2. The uncertainty and MSE of the fusion results of different models with Dataset , FLI is the flight test data

Model	Uncertainty-Cx	Uncertainty-Cy	Uncertainty-Cz	MSE
FLI	0.3394	2.1005	1.0786	\
Lin [13]	0.1791	1.5662	0.2513	2.523e-4
He [14]	0.1101	1.5630	0.1476	6.567e-4
Hu [6]	0.1897	1.2649	0.1891	8.259e-4
LGFNet w/o SW and Att	0.1168	0.9550	0.1205	5.667e-4
LGFNet w/o SW	0.1073	0.8796	0.1127	5.167e-4
LGFNet	**0.0730**	**0.7672**	**0.1128**	5.132e-4

Table 3. The uncertainty of the fusion results of different models with Dataset , WT is the wind tunnel test data

Model	Uncertainty-Cx	Uncertainty-Cy	Uncertainty-Cz
WT	1. 1398	5.1654	1. 0354
Lin [13]	1.0043	4.5880	0.7178
He [14]	1.5069	4.5574	2.1242
Hu [6]	0.9015	**4.2018**	0.7900
LGFNet	**0.8125**	4.9945	**0.6821**

Ablation Experiments

We conducted an ablation study comparing the complete LGFNet, LGFNet without the sliding window (w/o SW), and LGFNet without both SW and self-attention (w/o SW & Att), averaging results across all random seeds. As shown in Figure 3a, the complete LGFNet optimally integrates the trends of both FLI and CFD data. In contrast, removing the SW degrades fusion performance, and removing both modules fails to fuse the data effectively. Furthermore, quantitative results in Table 2 confirm that the complete LGFNet achieves the lowest uncertainty and MSE, demonstrating the necessity and effectiveness of each proposed module.

*Corresponding Author, E. Stavropoulos-Vasilakis evangelos.stavropoulos-vasilakis@city.ac.uk

Proceedings of the 1st international Symposium on AI and Fluid Mechanics
Paper No [leave blank]

Multi-Fidelity Data Fusion Method for Aerodynamic Heating Prediction of Hypersonic Vehicles

[1]Zhiyu Duan*;[1]Wanshu Li; [1]Wenwen Zhao; [1]Weifang Chen
1School of Aeronautics and Astronautics, Zhejiang University, Hangzhou, China;

Abstract

Accurate prediction of aerodynamic heating remains a critical challenge in hypersonic vehicle design. Current methodologies for acquiring heating data including computational fluid dynamics (CFD) simulations and wind tunnel experiments involve inherent trade-offs between measurement accuracy, spatial resolution, and implementation costs. Conventional multi-fidelity modeling approaches fail to ensure both comprehensive surface prediction improvements and reliable extrapolation to novel flight conditions due to experimental data scarcity. This study presents an augmented data fusion framework that synergizes data enhancement strategies with an innovative Multi-fidelity U-Net (MF-UNet) architecture. The proposed framework achieves dual advancements through expanding limited experimental datasets via systematic data augmentation to enhance extrapolation robustness, coupled with developing an optimized multi-fidelity mapping mechanism via MF-UNet for high-precision heat flux reconstruction. Validation on a hypersonic bi-ellipsoid configuration demonstrates the framework's effectiveness in integrating three sparse experimental datasets to generate complete surface heating profiles. Experimental results show significant improvements over baseline CFD solutions, achieving surface-averaged NRMSE below 3% compared with experimental measurements. The methodology successfully addresses challenges in multi-fidelity integration while enabling full-surface extrapolation, providing an engineering-viable solution for aerodynamic heating analysis.

Keywords: Data fusion; Aerodynamic heating; Multi-fidelity modeling; High-accuracy reconstruction of wall physical quantities

Introduction

Hypersonic flight generates severe aerodynamic heating on vehicle surfaces, particularly near stagnation regions, leading edges, and shock-interaction zones. Accurate heat-flux prediction is therefore essential for thermal protection system design: underprediction may threaten flight safety, whereas overprediction leads to unnecessary structural mass and reduced payload capacity [1-4]. Existing aerothermal prediction approaches mainly include empirical correlations, CFD simulations, and wind-tunnel experiments. Empirical methods are efficient but limited for complex configurations; CFD provides full-field heat-flux distributions but may suffer from model and grid uncertainties; wind-tunnel measurements offer higher reliability at sensor locations but are usually sparse, costly, and difficult to extend to untested flight conditions [5-10].

Multifidelity learning provides a promising way to combine low-fidelity CFD fields with limited high-fidelity experimental data. However, existing multifidelity models often focus on pointwise correction or require sufficient experimental samples, making it difficult to achieve accurate full-surface heat-flux reconstruction under new inflow conditions [11-16]. To address this issue, this study proposes a data-augmented multifidelity U-Net framework for aerodynamic heating prediction of hypersonic vehicles. The method first expands sparse wind-tunnel measurements by introducing CFD-informed virtual points in high-gradient heating regions, and then reconstructs full-surface heat-flux distributions through a hybrid-loss MF-UNet that preserves CFD-derived physical trends while correcting local prediction errors. Validation on a hypersonic double-ellipsoid configuration demonstrates that the proposed framework can effectively fuse sparse experimental data and CFD fields to obtain accurate and physically consistent aerodynamic heating predictions.

Methodology

The proposed method aims to reconstruct high-fidelity full-surface heat-flux distributions by fusing sparse wind-tunnel measurements with full-field CFD data. As shown in Figure 1, The framework contains two main stages. First, CFD-informed data augmentation is performed to expand limited experimental measurements under different inflow conditions. Second, the augmented high-fidelity data and low-fidelity CFD fields are integrated through an MF-UNet model for complete surface heat-flux reconstruction.

*Corresponding Author, Zhiyu Duan, 12424076@zju.edu.cn

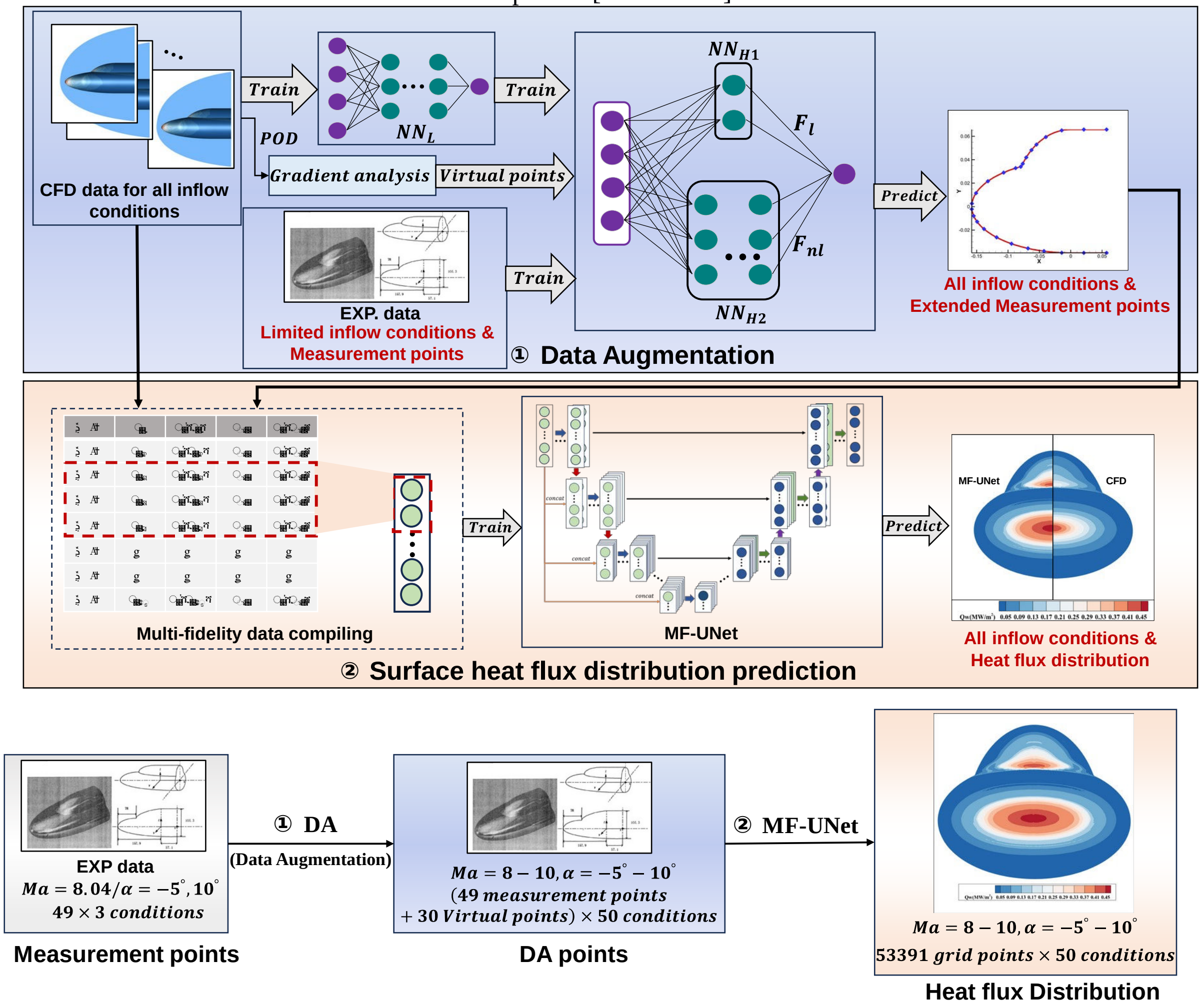

Figure 1 Technical approach for heat flux distribution prediction utilizing MF-UNet

The CFD solution is regarded as low-fidelity data because it provides complete surface heat-flux distributions but may contain model-form errors. As shown in Figure 2, a low-fidelity DNN is first trained using CFD samples, where the input variables include inflow parameters, surface coordinates, and wall-temperature-related features, and the output is the CFD heat flux. To improve the spatial coverage of sparse wind-tunnel measurements, POD is applied to the CFD heat-flux database to extract the dominant thermal mode. Virtual measurement points are then selected in high-gradient regions of this dominant mode, where rapid heat-flux variation is expected. A multifidelity DNN is used to map the low-fidelity CFD prediction to high-fidelity experimental heat flux at both physical and virtual measurement points. In this way, the original sparse experimental dataset is expanded while preserving the main CFD-derived thermal distribution features.

*Corresponding Author, Zhiyu Duan, 12424076@zju.edu.cn

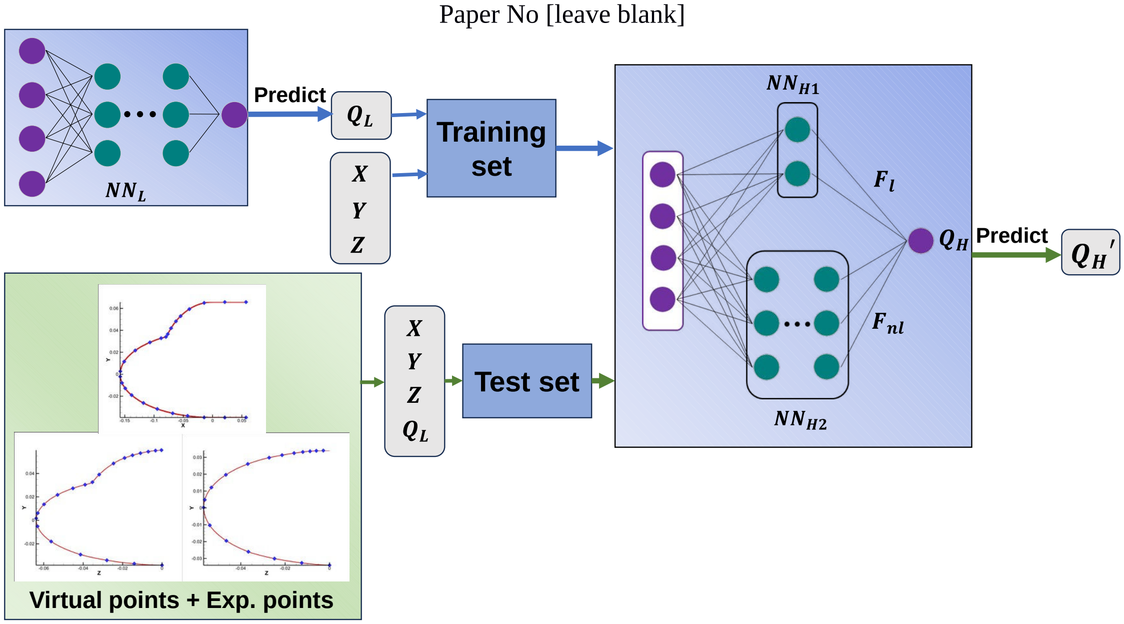

Figure 2 Training process of the low-fidelity DNN

Although the augmented measurements improve the coverage of critical regions, they still do not directly provide a complete surface heat-flux field. Therefore, an MF-UNet model is developed to learn the mapping between sparse high-fidelity measurements and full-field low-fidelity CFD distributions. As shown in Figure 3, The multifidelity input is organized by linking each high-fidelity point with its neighboring CFD samples, which forms a local receptive-field structure suitable for one-dimensional convolution. As shown in Figure 4, The MF-UNet adopts an encoder–decoder architecture with skip connections to extract multiscale thermal features while retaining local heat-flux peaks and gradient information. To maintain physical consistency, the model is trained using a hybrid loss function:

$$Loss = \sqrt{\frac{1}{N_L}\sum_{i=1}^{N_L}(\hat{Q}_{L,i} - Q_{L,i})^2} + \theta\sqrt{\frac{1}{N_H}\sum_{j=1}^{N_H}(\hat{Q}_{H,j} - Q_{H,j})^2}$$

The first term constrains the reconstructed field using the global CFD heat-flux distribution, while the second term corrects the prediction using high-fidelity wind-tunnel measurements. Through this design, the proposed method can correct local CFD errors while preserving the physically reasonable heat-flux distribution trend over the entire surface.

*Corresponding Author, Zhiyu Duan, 12424076@zju.edu.cn

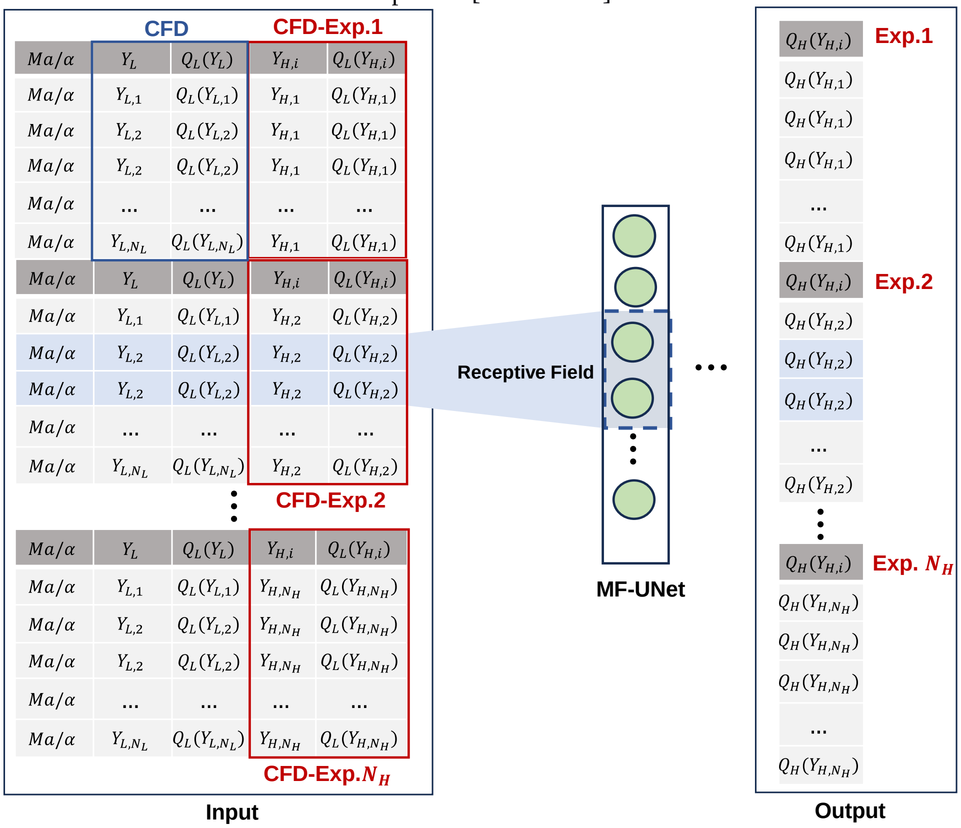

Figure 3 Multi-fidelity data compiling

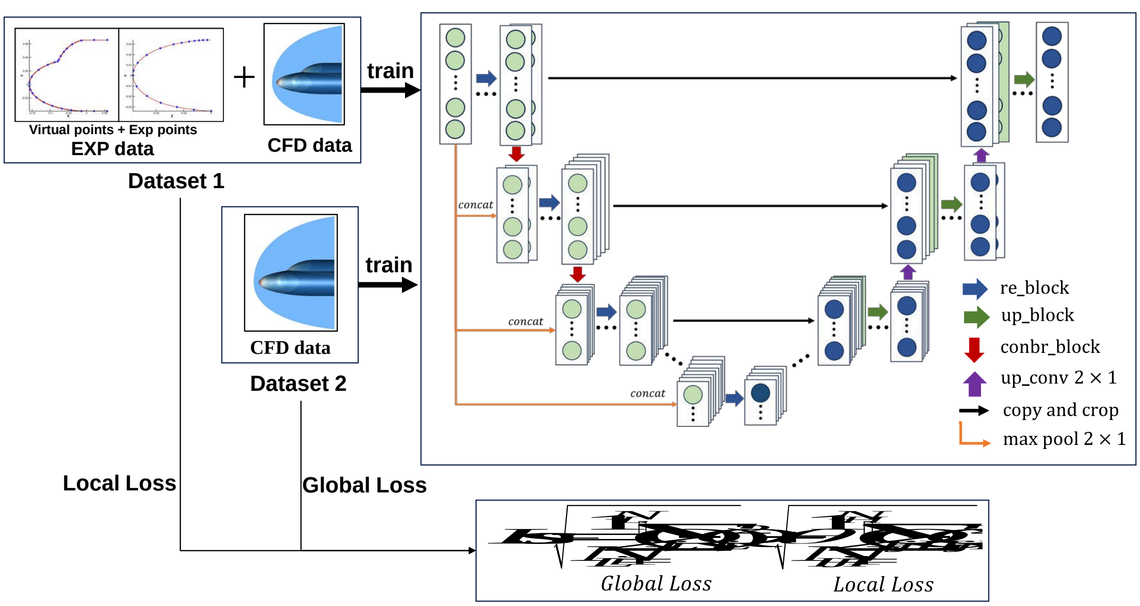

Figure 4 MF-UNet network architecture and training method

Results

The proposed framework was evaluated on a hypersonic double-ellipsoid configuration using CFD simulations and wind-tunnel heat-flux measurements. The CFD model provides full-surface heat-flux distributions, whereas the experimental data are available only at sparse measurement locations. Therefore, the evaluation focuses on three aspects: the discrepancy between CFD and experimental data, the accuracy of CFD-informed data augmentation, and the full-surface reconstruction capability of the proposed MF-UNet.

*Corresponding Author, Zhiyu Duan, 12424076@zju.edu.cn

As shown in Figure 5, the CFD results reproduce the overall aerodynamic heating distribution of the double-ellipsoid configuration, including the high heat-flux region near the nose and the heating variation along the body surface. However, clear discrepancies are observed between CFD and wind-tunnel measurements, especially near the stagnation region and the intersection line of the double ellipsoid. These regions are strongly affected by shock-wave and boundary-layer interactions, where conventional CFD tends to underpredict local heat-flux peaks. This comparison confirms that CFD alone can provide the global thermal trend but cannot fully recover the high-fidelity heating response at critical locations.

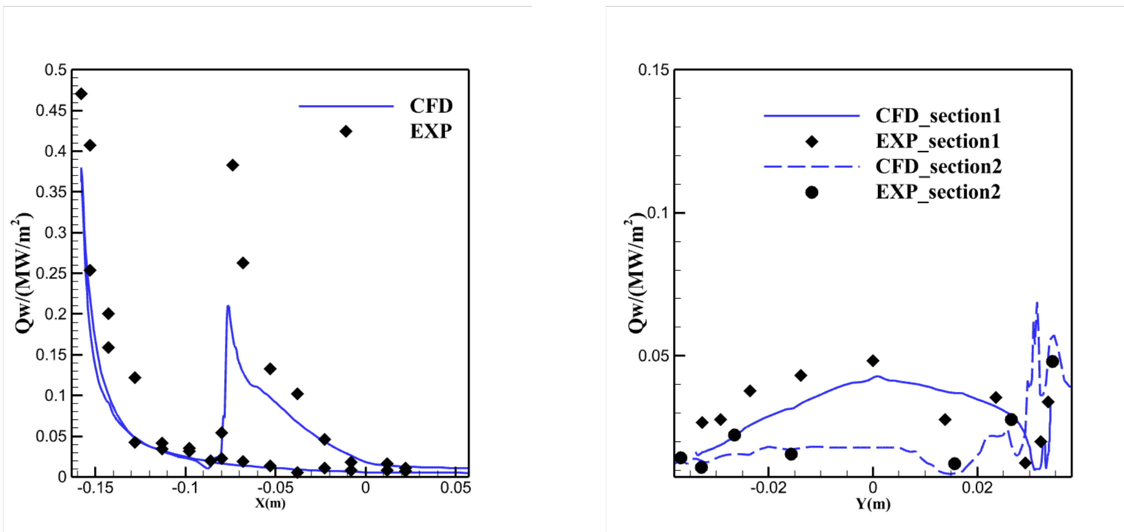

(a) Surface meridian **(b) Cross section1 and 2**

Figure 5 Comparison between CFD result and wind tunnel experimental result

The CFD-informed data augmentation strategy was first evaluated at sparse measurement locations. The low-fidelity DNN was trained using CFD data to learn the relationship between inflow parameters, surface coordinates, and heat flux. Then, the multifidelity DNN corrected the CFD-based prediction using wind-tunnel measurements. As shown in Figure 6, the results show that the augmented heat-flux values agree well with the experimental measurements under both angle-of-attack and Mach-number generalization cases. For α-generalization, the NRMSE values are 0.1700%, 0.1900%, and 0.2200% at α = 0° for the surface meridian, cross section 1, and cross section 2, respectively. At α = 10°, the corresponding errors are 0.1300%, 0.1400%, and 0.2700%. For Ma = 10.02, the errors are 0.1200%, 0.2400%, and 0.3100%. These results indicate that the data augmentation module can accurately infer high-fidelity heat-flux values at both tested and untested inflow conditions.

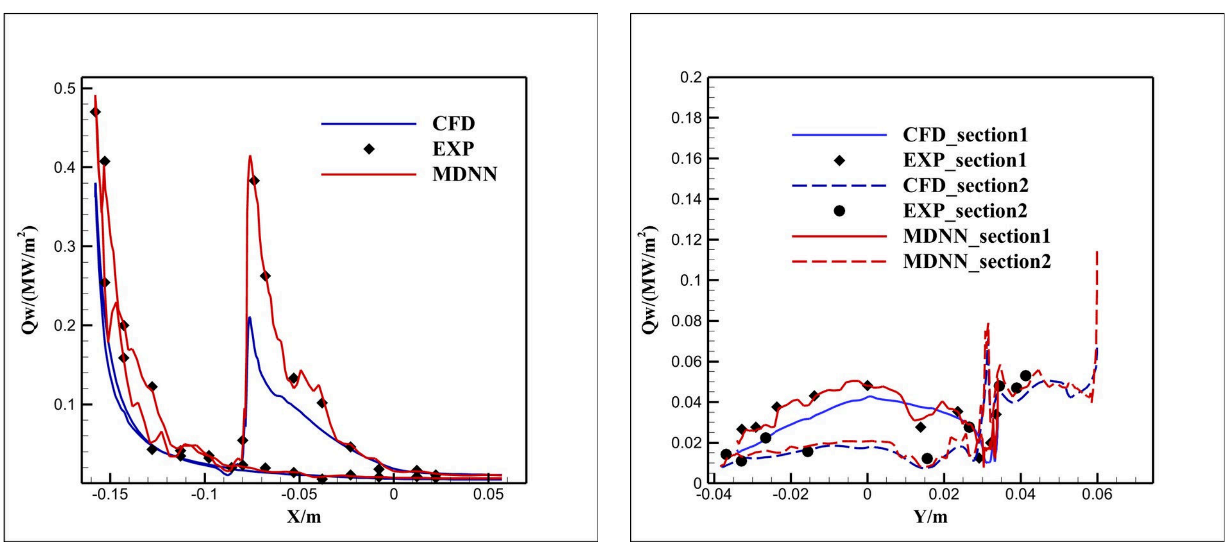

(a) Surface meridian **(b) Cross section1 and 2**

Figure 6 Comparison of prediction results from the multi-fidelity DNN network architecture,

*Corresponding Author, Zhiyu Duan, 12424076@zju.edu.cn

In addition, virtual measurement points selected from high-gradient regions of the dominant POD mode improve the coverage of critical heating regions. As shown in Figure 7, the augmented points are mainly distributed near locations with rapid heat-flux variation, which helps the subsequent reconstruction model better capture local peaks and steep gradients.

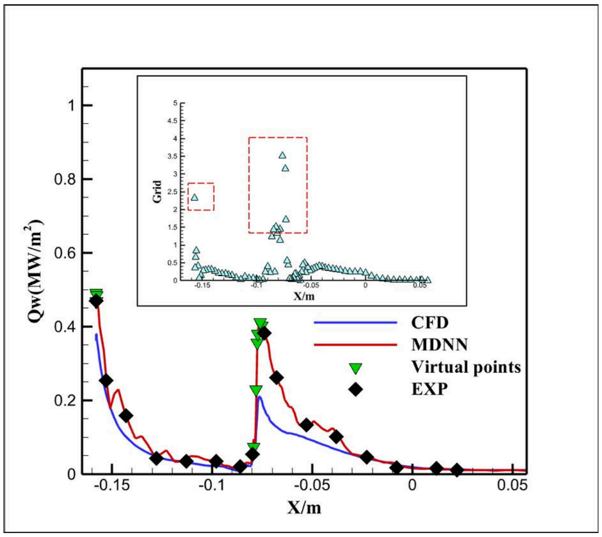

(a) Surface meridian(leeward)

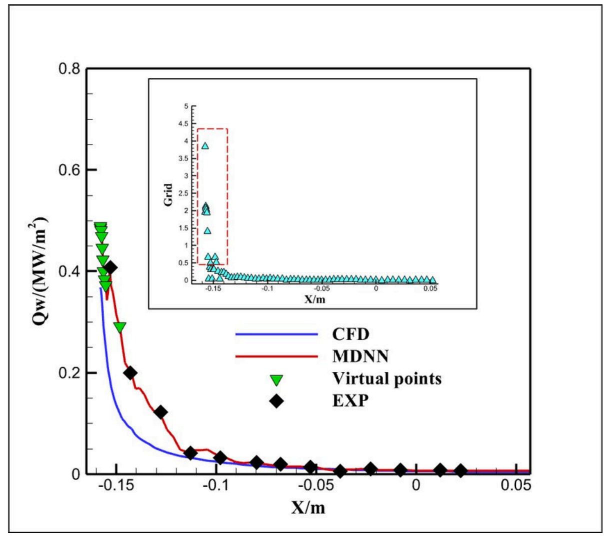

(b) Surface meridian(windward)

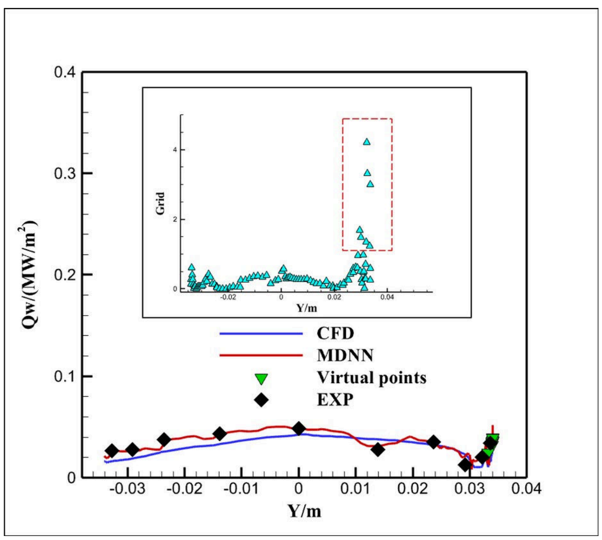

(c) Cross section1

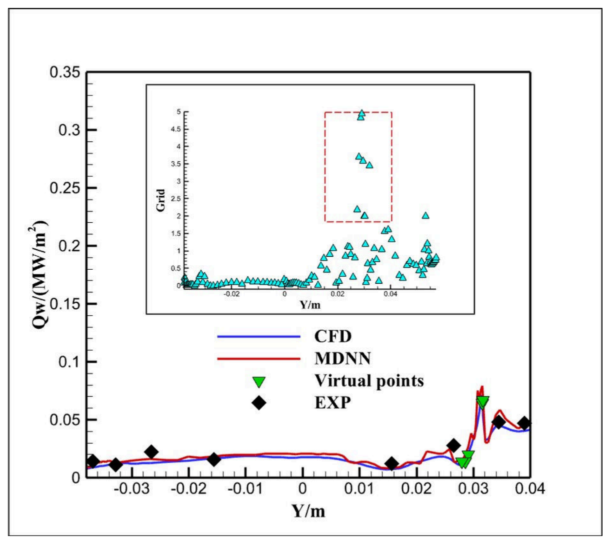

(d) Cross section2

Figure 7 Comparison of experimental data augment results including virtual points,

After data augmentation, the MF-UNet was used to reconstruct the complete surface heat-flux distribution. As shown in Figure 8, the predicted contours show that the proposed model preserves the global CFD-derived heating pattern while correcting local heat-flux errors near critical regions. In particular, the model captures the stagnation-point heating and the secondary heat-flux rise downstream of the ellipsoid junction, which are difficult to reproduce accurately using CFD alone.

*Corresponding Author, Zhiyu Duan, 12424076@zju.edu.cn

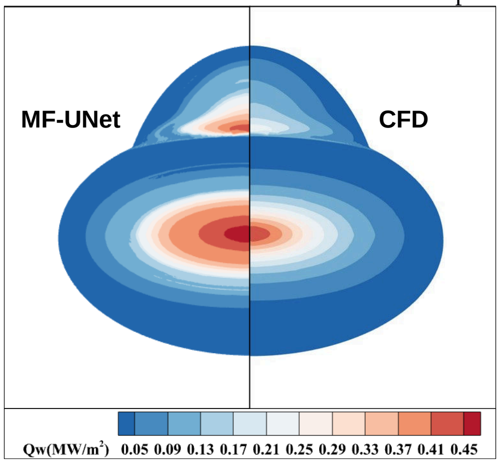

(a) Heat flux contours

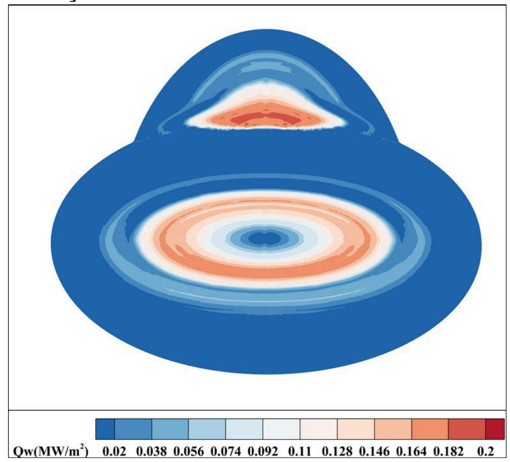

(b) Absolute error between MF-UNet and CFD

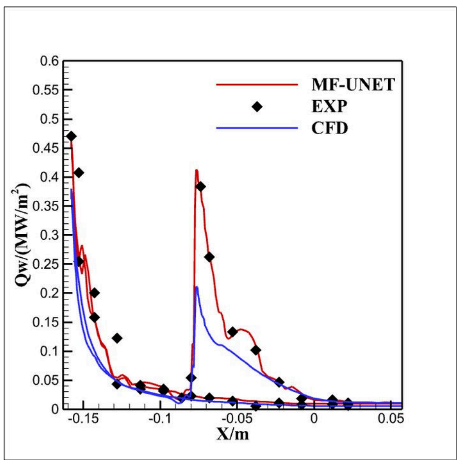

(c) Surface meridian

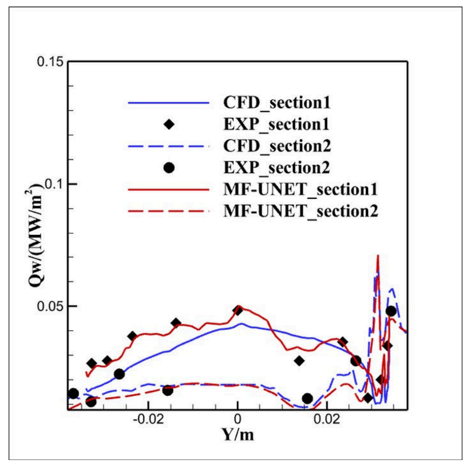

(d) Cross section1 and 2

Figure 8 Generalization prediction performance of MF-UNet for angle of attack without data augmentation,

The comparison between CFD, MF-UNet without virtual points, and MF-UNet with virtual points further demonstrates the contribution of the proposed data augmentation strategy. For the α = 0° case, as shown in Figure 9, the CFD result gives an NRMSE of 17.9600%, whereas MF-UNet without virtual points reduces the error to 0.6700%. After introducing virtual points, the error further decreases to 0.4400%.

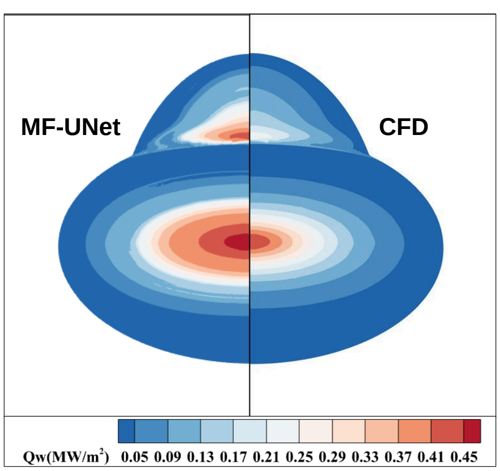

(a) Heat flux contours

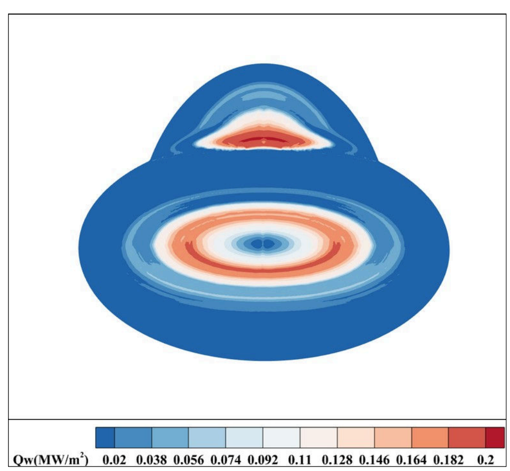

(b) Absolute error between MF-UNet and CFD

*Corresponding Author, Zhiyu Duan, 12424076@zju.edu.cn

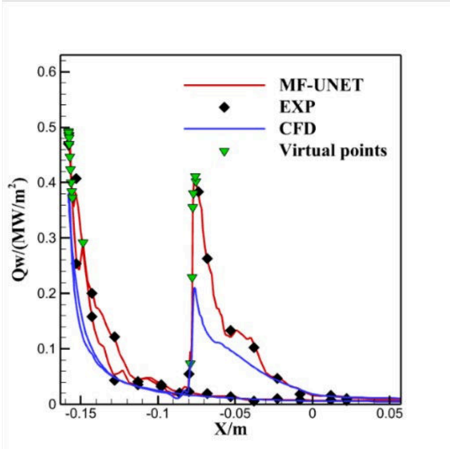

(c) Surface meridian

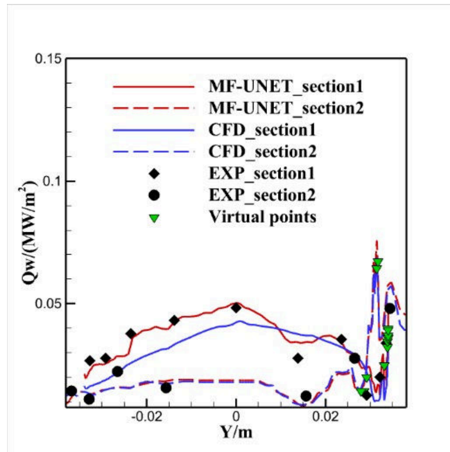

(d) Cross section1 and 2

Figure 9 Generalization prediction performance of MF-UNet for angle of attack with data augmentation,

Conclusion

A data-augmented multifidelity U-Net framework is developed for aerodynamic heating prediction of hypersonic vehicles. The method combines sparse wind-tunnel measurements with full-field CFD data through two key steps: CFD-informed data augmentation with virtual measurement points in high-gradient regions, and full-surface heat-flux reconstruction using a hybrid-loss MF-UNet. By integrating global CFD-derived thermal patterns with localized high-fidelity experimental information, the proposed framework achieves accurate and physically consistent heat-flux prediction over the entire surface. Validation on a hypersonic double-ellipsoid configuration demonstrates robust performance under angle-of-attack and Mach-number extrapolation, with substantial error reduction compared with CFD alone. The framework provides a practical and efficient approach for aerodynamic heating assessment when experimental data are sparse.

References

1.McNamara, J. J., and Friedmann, P. P. (2011). Aeroelastic and aerothermoelastic analysis in hypersonic flow: past, present, and future. *AIAA Journal*, 49(6), 1089-1122.

2.Robinson, J. (2011). An overview of NASA’s integrated design and engineering analysis (IDEA) environment. *17th AIAA International Space Planes and Hypersonic Systems and Technologies Conference*, AIAA Paper 2011-2392.

3.Eyi, S., Hanquist, K. M., and Boyd, I. D. (2019). Aerothermodynamic design optimization of hypersonic vehicles. *Journal of Thermophysics and Heat Transfer*, 33(2), 392-406.

4.Gonzalez, C., Castillo, J., and Shirin, A. (2025). Hypersonic heat flux prediction and validation. *AIAA SCITECH 2025 Forum*, AIAA Paper 2025-2634.

5.Li, T., Guo, L., Yang, Z., Sun, G., Zeng, L., Liu, S., and Wang, Y. (2022). An automatic shape-aware method for predicting heat flux of supersonic aircraft based on a deep learning approach. *Physics of Fluids*, 34(7).

6.Fay, J., and Riddell, F. R. (1958). Theory of stagnation point heat transfer in dissociated air. *Journal of the Aerospace Sciences*, 25(2), 73-85.

7.Eckert, E. R. G. (1955). Engineering relations for friction and heat transfer to surfaces in high velocity flow. *Journal of the Aeronautical Sciences*, 22(8), 585-587.

8.Qu, F., Chen, J., Sun, D., Bai, J., and Zuo, G. (2019). A grid strategy for predicting the space plane’s hypersonic aerodynamic heating loads. *Aerospace Science and Technology*, 86, 659-670.

9.Kumar, R., and Sahoo, N. (2013). Dynamic calibration of a coaxial thermocouples for short duration transient measurements. *Journal of Heat Transfer*, 135(12), 124502.

10.Hamadi, D., Garnier, B., Willaime, H., Monti, F., and Peerhossaini, H. (2012). A novel thin-film temperature and heat-flux microsensor for heat transfer measurements in microchannels. *Lab on a Chip*, 12(3), 652-658.

*Corresponding Author, Zhiyu Duan, 12424076@zju.edu.cn

11.Chen, X. (2011). *Experimental technique study of heat transfer measurement on sharp leading edges* (Ph.D. thesis). National University of Defense Technology, Changsha, China.

12.Zhu, G., Nie, C., Cao, Z., and Yuan, Y. (2019). Research progress in aerodynamic thermal environment testing and measurement technology. *Journal of Experiments in Fluid Mechanics*, 33(2), 1-10.

13.Zhang, R., Li, X., Yao, W., Zheng, X., Wang, N., and Sun, J. (2024). Implicitly physics-informed multifidelity physical field data fusion method based on Taylor modal decomposition. *Advanced Engineering Informatics*, 62, 102738.

14.Castanedo, F. (2013). A review of data fusion techniques. *Scientific World Journal*, 2013, 704504.

15.Leifsson, L., and Koziel, S. (2010). Multifidelity design optimization of transonic airfoils using physics-based surrogate modeling and shape-preserving response prediction. *Journal of Computational Science*, 1(2), 98-106.

16.Han, Z. H., Zhang, Y., Song, C. X., and Zhang, K. S. (2017). Weighted gradient-enhanced kriging for high-dimensional surrogate modeling and design optimization. *AIAA Journal*, 55(12), 4330-4346.

*Corresponding Author, Zhiyu Duan, 12424076@zju.edu.cn